Int. J. Electrochem. Sci., 14 **(2019)** 10410 – 10419, doi: 10.20964/2019.11.42

International Journal of
ELECTROCHEMICAL
SCIENCE
www.electrochemsci.org

Facile synthesis of Co-doped VO_2 (B) as the Cathode Material for Lithium-Ion Batteries with Enhanced Electrochemical Performance

Shichang Han[1,*], *Zhaoming Huang*[1], *Jing Xu*[1], *Weiwei Han*[2] ,*Tian Chen*[1].

[1] College of Mechanical Engineering, Wanjiang University of Technology, Ma'anshan, 243031, China
[2] School of Energy and Environment, Anhui University of Technology, Ma'anshan, 243002, China
[*]E-mail: hanscahut@163.com

Received: 8 July 2019 / *Accepted:* 26 August 2019 / *Published:* 7 October 2019

Recently, VO_2 (B) has received increasing attention due to its unique layered structure in lithium-ion batteries (LIBs). However, little study is focused on the effect of transition metal doping on its electrochemical performance. Herein, Co-doped VO_2 (B) electrode materials were fabricated via a facile and controllable hydrothermal method. The as-prepared electrode show an excellent electrochemical performance. When employed as cathodes for LIBs, the capacity retention of the $Co_{0.02}V_{0.98}O_2$ (B) can keeps 54.1% after 100 cycles at 0.1 C, i.e., 36 mA h g^{-1} larger than that for the pristine. The good electrochemical performance of the composites indicates their high potential as an electrode material for LIBs.

Keywords: Lithium-ion battery; Cathode material; VO_2 (B); Co doping

1. INTRODUCTION

Electrochemical energy storage has become a key technology because of the exhaust of traditional nonrenewable fossil resources and serious environment pollution [1-4]. Comparing with conventional storage devices, lithium ion secondary batteries are attractive energy storage technique due to its long cycle life, high capacity and environmentally friendly characteristics [5-8]. The cathode material is one of the most important components for LIBs; meanwhile, it is also the biggest bottlenecks, restricting the practical application of LIBs. The typical layered transition metal oxides of V_6O_{13}, VO_2 and V_2O_5 as cathode materials have been extensively studied in the past decades, and regarded as a promising electrode material for LIBs [9-11].

In particular, the metastable VO_2 (B) formed from layered structures of shared VO_6 octahedra, thus forming abundant one-dimensional tunnels along the b axis [12-15]. This kind of structure has high theoretical capacity (324 mA h g^{-1} for one Li per VO_2) than other types of vanadium oxides [12, 14]. And it possesses rapid lithium ion diffusion rate and ample sources [16-18]. But this material of electrochemical performance synthesized in the laboratory that not achieve the desired effect. Some studies report the actual capacity less than half the theoretical capacity and the charge-discharge cycle performance is also not particularly desirable [19-20]. It is thought that the crystal defect causes this phenomenon. It is well known that doping, carbon coating and nanocrystallization are three common methods of material modification. For instance, some researchers have improved electrochemical performance by changing the morphology, such as nanorods, nanowires, nanobelts and nanospheres have been prepared [21-24]. On the other hand, modification with carbon nanomaterials can also be used to obtain high electrochemical properties. In this regard, we will consider using carbon nanotubes developed in our laboratory to modify VO_2 (B) [25, 26]. Nonetheless, the electrochemical performance has been improved to some extent, but the effect is not very ideal. To the best of our knowledge, Transition metal ion doping is a practical way to improve material properties. Zou et al. [27] synthesized Fe-doped VO_2 (B) cathode material by one step hydrothermal synthesis method. The $Fe_{0.03}$ VO_2 (B) sample showed the best lithium storage performance with initial discharge capacity of 306 mA h g^{-1} at the current density of 0.1 C in the voltage range from 1.5 to 4.0 V, but its charge-discharge cycle performance is worse. So it is urged to develop new cathode material to make up the energy storage equipment.

In this study, Co-doped VO_2 (B) were prepared by one step hydrothermal synthesis method for the first time, which were employed as cathode material for LIBs. Microstructure and electrochemical properties of Co doped VO_2 (B) were investigated in order to discuss the effects of cobalt dopant on the doped material.

2. EXPERIMENT

All the raw materials were analytically pure. The solvothermal was used to synthesize $Co_xV_{1-x}O_2$ (B) (x=0, 0.01, 0.02, 0.03, where x represents the molar ratio of Co). 1.25 g $C_2H_2O_4{\cdot}2H_2O$ and 0.4 g V_2O_5 were magnetically stirred with 20 ml deionized water in a beaker at 80 °C to obtain VOC_2O_4, and then a suitable amount of $Co(NO_3)_2{\cdot}6H_2O$, 20 ml of the VOC_2O_4 solution and 3 ml of 30% H_2O_2 were added into a 100 ml inner lining of reaction kettle pre-filled with 30 ml of deionized water. After stirring for 10 minutes, the autoclave was sealed and maintained at 160 °C for 24 h in an oven, followed by natural cooling to room temperature. Finally, the calcination was carried out at 350 °C in nitrogen atmosphere to obtain a final product, which were labeled as Co_1, Co_2, Co_3 and Co_4, respectively.

The phase of samples were analyzed by a Philips X'pert Pro diffractometer with a Cu Kα radiation source (λ = 0.154 nm) at the scanning rate of 6 °/min. Fourier transform infrared spectroscopy (FT-IR) pattern of the solid samples was measured using KBr pellet technique and recorded on a Nicolet 6700 spectrometer from 4000 to 400 cm^{-1} with a resolution of 4cm^{-1}. The morphology and dimensions of the products were observed by Field emission scanning electron microscopy (FESEM, Hitachi S-4800). Quantitative analysis of samples using an energy diffusion spectrometer (Oxford, UK, INCAIE 350). X-ray photoelectron spectroscopy (XPS) measurements were carried out with an ESCALAB

250Xi spectrometer using Al Kα (1486.6eV) X-ray source. The EIS and CV of the cathode materials were texted using electrochemical workstations (CHI860D) by Beijing Huakeputian Technology. The coin cell was assembled in a glove box using Shenzhen (BTS-5 V-5 mA) test system to test the charge-discharge cycle of the samples.

3. RESULTS AND DISCUSSION

Fig. 1 exhibits the phase structure of different Co-doped amounts. **Fig. 1(a)** shows that the products are basically in line with the monoclinic VO_2 (B) standard card (JCPDF NO.71-2235) [28] and no impurity phase is detected with the change in the amount of doping, indicating that doping did not have effect on the phase structure. Note that there are changes in the XRD pattern with the addition of cobalt atoms (**Fig. 1(b)**). We observe the change of the Bragg peak located at 2θ=25.34°, the diffraction peak shifted to low angle compared to undoped, and the deviation angle increases with the doping amount. The crystallite size for the VO_2 (B)was determined by the MDI Jade software (**Table 1.**). The results show that the cell volume of amounts as the Co content increases. This is due to the substitution of Co^{2+} (0.0645 nm) for V^{4+} (0.058 nm). More structure information about Co-doped VO_2 (B) composites was provided by FTIR in **Fig. 1(c)**. Among them, the peaks at 1610 cm^{-1} are attributed to C=C bonds [29], 1000 cm^{-1} corresponds to symmetric stretching of the νs (V^{4+}=O) bonds, and 543 cm^{-1} corresponds to the absorption peak of V-O-V bond [30].

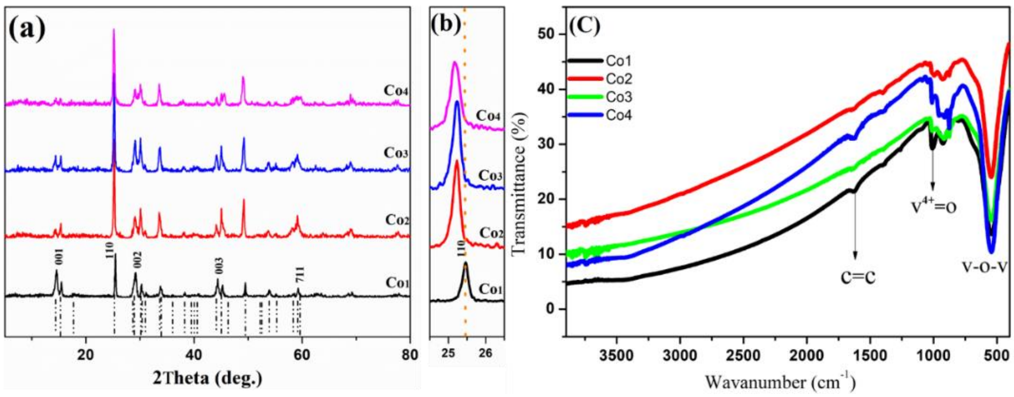

Figure 1. (a) XRD patterns of different doped samples; (b) XRD patterns of (110) crystal plane; (c) FTIR patterns of different doped samples

Table 1. Lattice constants and cell volumes for different doped samples.

Specimen	*a*(Å)	*b*(Å)	*c*(Å)	*V*($Å^3$)
Co_1	12.0396	3.6737	6.4199	271.79
Co_2	12.0521	3.6961	6.3951	273.00
Co_3	12.0638	3.6986	6.4143	274.22
Co_4	12.0685	3.7002	6.4226	274.39

The chemical composition of as-obtained samples was revealed by means of the Energy-Dispersive X-ray Spectrometer (EDS) attached to FESEM in **Fig. 2**. it shows that the relative atomic mass of Co increases with the doping amount.

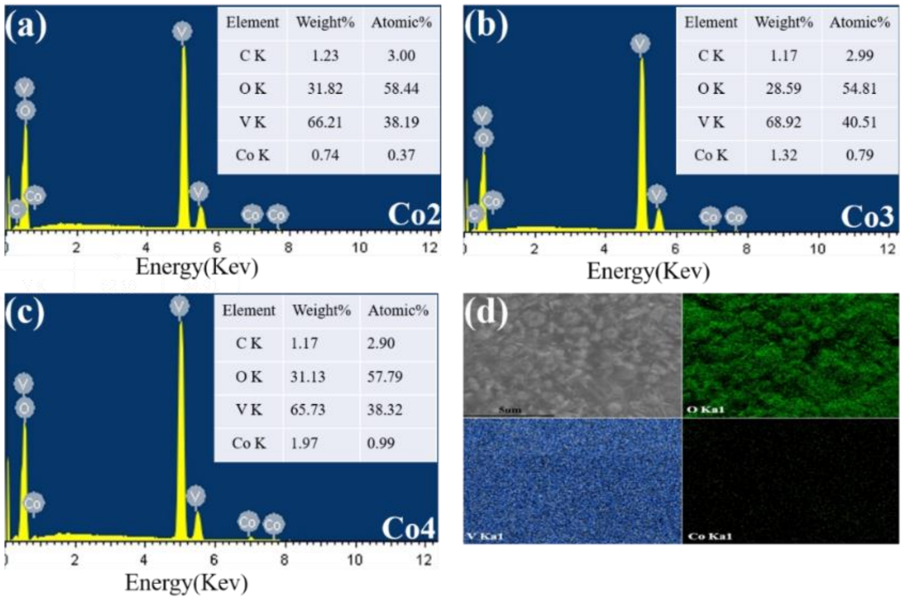

Figure 2. EDS of different doped samples(a) Co_2 (b) Co_3 (c) Co_4. (d) element mapping images of V, O, and Co of $Co_xV_{1-x}O_2$(B).

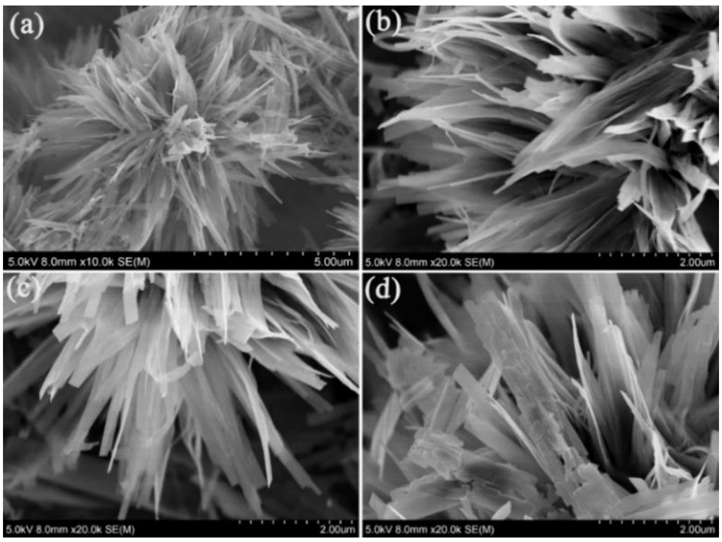

Figure 3. FESEM images of different doped samples (a) Co_1 (b) Co_2 (c) Co_3 (d) Co_4.

The results show that Co has been successfully occupy the position of V in the sample. **Fig. 3** shows the SEM images of the Co-doped VO_2 (B) composites. It can be seen from FESEM images that the microstructure of the sample has not changed much before and after doping. Like a cluster of flowers are composed of end-connected nanosheets. These suggest that the addition of cobalt nitrate did not change the crystal growth environment. **Fig. 3(a)** is an undoped sample, the average length is 4.0 µm. **Fig. 2(a-c)** are Co_2, Co_3, and Co_4, respectively.

The growth pattern is changed with the increase of Co-doped amounts. The sheets become wider and the particle size decreases. As we know, the particle size is larger and the specific surface area is smaller. More surface facilitates the intercalation and de-intercalation of lithium ions, which can improve the electrochemical performance.

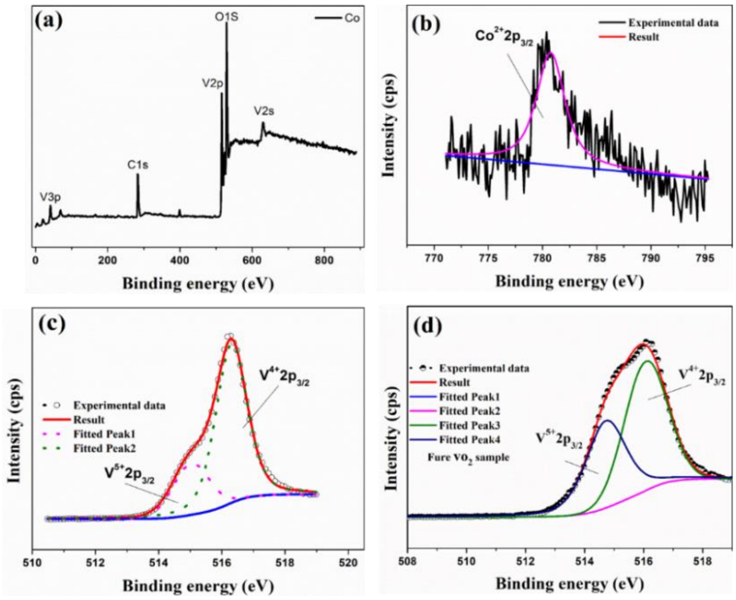

Figure 4. (a) XPS survey spectrum of the Co_3 sample; (b) high-resolution spectrum of Co^{2+} 2p core-level spectrum for Co_3 sample; (c) high-resolution spectrum of V 2p core-level spectrum for Co_3 sample; (d) high-resolution spectrum of V 2p core-level spectrum for pure VO_2(B) sample.

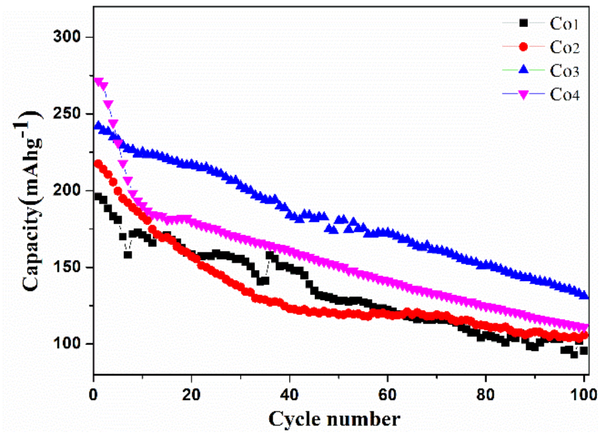

Figure 5. The cyclic performance of different Co-doped samples Co_1, Co_2, Co_3 and Co_4, at the current density of 32.4 mA g^{-1} in 1.5−4.0 V.

X-ray photoelectron spectroscopy was used to provide more information on structural properties. The XPS full scan spectrum of Co-VO_2 (B) is shown in **Fig. 4(a)**. The peaks situated at 285 eV, 400 eV, 515 eV and 532 eV are ascribed to C 1s, N 1s, V 2p and O 1s energy level, respectively [31,32], which indicates that there are elements of O, V, and C in the sample. As shown in **Fig. 4(b)**, The peaks situated at 780.75eV, are ascribed to Co 2p energy level [33], The lines in the V $2p_{3/2}$ spectra of VO_2 (B) (**Fig. 4(c, d)**) were broad, ranging from 514 to 518 eV, indicative of mixed oxidation states of vanadium ions. By means of XPS-peak-differenating analysis, the V $2p_{3/2}$ spectrum contained two contributions at 515.04 eV and 516.30 eV, corresponding to $V^{5+}$and V^{4+} ions [34-37].

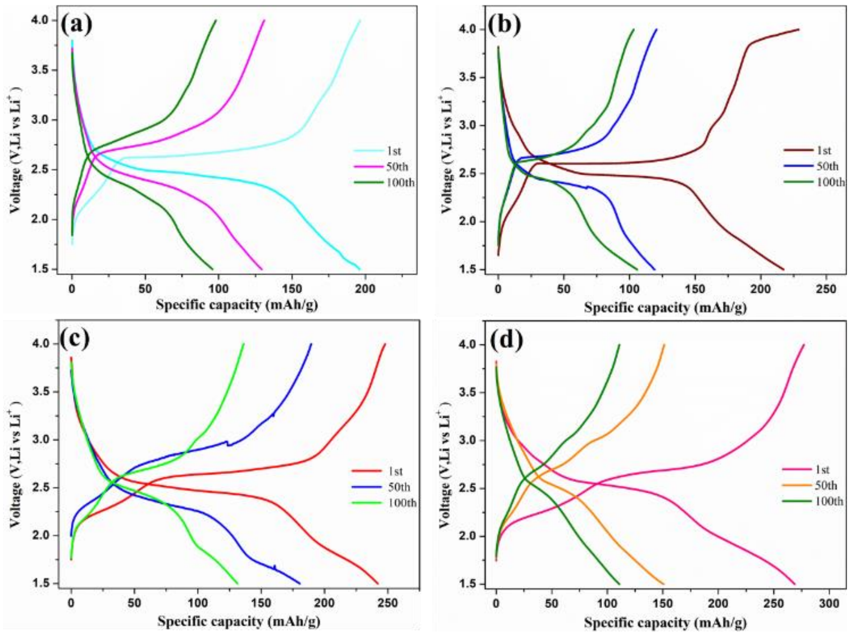

Figure 6. The charge and discharge curves of the first, fiftieth, and hundredth times for different doped samples (a) Co_1 (b) Co_2 (c) Co_3 (d) Co_4.

Table 2. The electrochemical performance of the Co-doped VO_2(B) with Other Reported VO_2-Based Electrodes.

cathode material	current density ($mAh\cdot g^{-1}$)	initial discharge capacity ($mAh\cdot g^{-1}$)	capacity retention	cycle number	Ref.
Co-doped VO_2(B)	32.4	242	54.1%	100	This work
Al-doped VO_2(B)	32.4	282	71.6%	50	40
Fe-doped VO_2(B)	32.4	306	64.7%	100	27
Ti-doped VO_2(B)	42	253	85.7%	51	41
Cu-doped VO_2(B)	42	317.1	73.8%	50	41

The discharge capacity and efficiency of the VO_2 (B) without and with Co as the cathode materials were evaluated for 100 cycles at the current density of 0.1 C, as displayed in Fig. 5. The discharge capacity significantly increases when cobalt ions are successfully incorporated, with the increasing of doping concentration. The first discharge specific capacity increased from 195 mA h g^{-1} to 271 mA h g^{-1} as x increased from 0 to 0.03. Notice that the cyclic performance does not increase with the doping content. For example, the cyclic capacity retention rate of Co_4 is about 40.5% after 100 cycles, which is lower than 48% of the sample without doping. By comparison, when x=0.02, it exhibits excellentelectrochemical properties. the capacity of Co_3 in the first discharge is 242 mA h g^{-1} with retention of 54.1% after 100 cycles, which is superior to the undoped counterpart. the other reported cathode materials [27,40,41] as showed in **Table 2**. The above analysis indicates that the synergetic effects of Co^{2+} doping could improve both the discharge capability and cycle stability of the VO_2 (B) nanomaterials.

The 1st, 50th and 100th galvanostatic charge-discharge measurements were performed in the voltage window of 2.0-4.0 V. The representative voltage profiles of the samples at a current density of 32.4 mA g^{-1} are shown in Fig. 6. The initial discharge curve consisted of one discharge plateaus, and the discharge plateau from 2.25 to 2.75V [38], which was attributed to the reduction of V^{5+} to V^{4+}. At the 50th and 100th discharge cycle, there were still one discharge plateaus, but the discharge plateau greatly decreases, and the discharge capacity has also dropped sharply.

Fig. 7 compares the CV curves of the samples under the scan rate of 0.1 mV s^{-1} in a voltage range of 1.5-4 V. It can be seen that the redox peaks in the CV were in good agreement with the plateaus observed in the voltage-capacity profiles. Potential differences of every redox reaction of $Co_xV_{1-x}O_2$(B) (x=0.01,0.02) samples are larger than the corresponding values of the pure VO_2 (B) sample. Co doping and pure VO_2 (B) samples exhibited a pair of redox peaks at about 2.3V and 2.9 V, which corresponds to the voltage platform of the discharge/charge process, respectively.

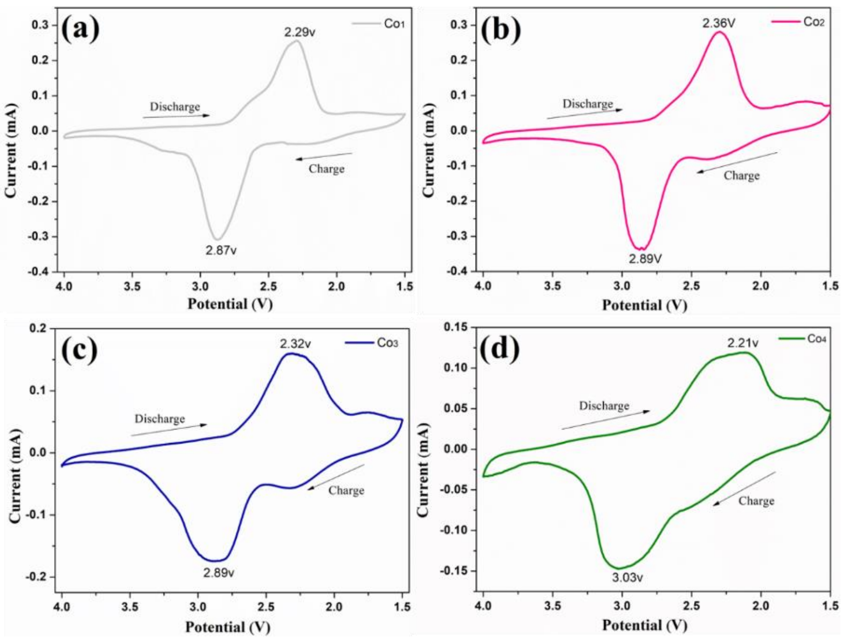

Figure 7. The cyclic voltammetry curves of 3 cycles for different doped samples (a) Co_1 (b) Co_2 (c) Co_3 (d) Co_4.

EIS is one of the most informative electrochemical analytical techniques to understand the kinetics of Li^+ intercalation/extraction process in intercalation compounds. EIS Nyquist plots of the pure VO_2 (B) and Co-doped VO_2 (B) samples measured at the 3th fully discharged state. The inset shows the expanded plots at the high frequency region in **Fig. 8**. The R_{ct} of the Co-doped VO_2 (B) samples are 615 Ω, 527 Ω, 649 Ω, respectively, which is lower than that of the pure VO_2 (B) sample (889 Ω), demonstrating that the material that containing Co^{2+} exhibits the better electrochemical kinetics.

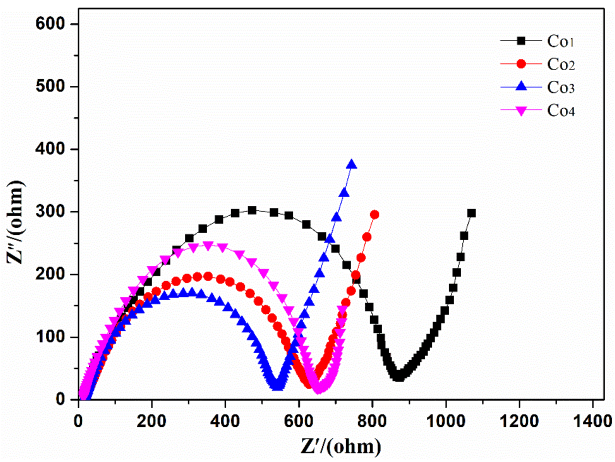

Figure 8 The electrochemical impedance spectroscopy of different doped samples of Co_1, Co_2, Co_3 and Co_4 after 3 cycles.

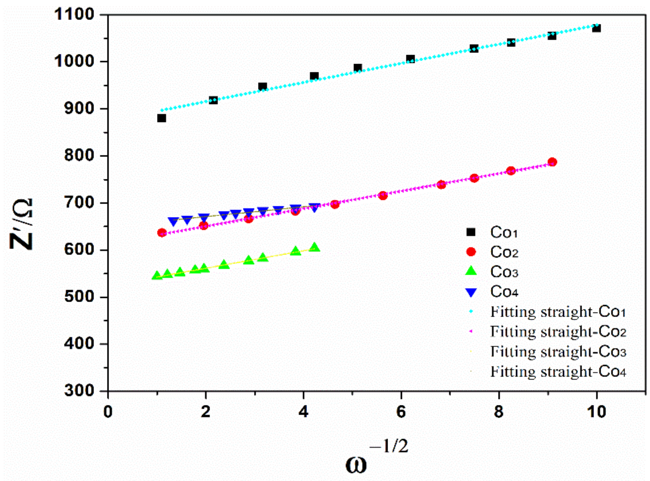

Figure 9. The relationship between Z' and $\omega^{-1/2}$ at low frequencies.

Fig. 9 shows the lithium-ion diffusion coefficients of samples, The values of D_{Li} can be calculated based on the following formula [39], when $Z' = R_s + R_{ct} + \sigma_w \omega^{-1/2}$:

$$D_{Li} = \frac{1}{2C_{Li}} \left[\frac{RT}{A \text{ n F } \sigma_{\omega}} \right]^2$$

where σ_w is Warburg impedance, F is Faraday constant, R_s is the resistance of the electrolyte and electrode material, R_{ct} is the charge transfer resistance, R is the gas constant, T is the absolute temperature, A is the surface area of the anode, n is the number of electrons per molecule during cycling, F is Faraday constant, C is the concentration of lithium ion, The relationship plot between Z' and $\omega^{-1/2}$ at low frequency region is shown in Fig. 9. D_{Li} were calculated to 8.04×10^{-15} cm^2 s^{-1} (Co_1), 9.51×10^{-15} cm^2 s^{-1} (Co_2), 9.59×10^{-15} cm^2 s^{-1} (Co_3) and 3.02×10^{-14} cm^2 s^{-1}(Co_4), respectively. The variation law of lithium-ion diffusion coefficient is alike to that of charge transfer resistance, further verifying that Co doping is an effective method to improve its electrochemical performances.

4. CONCLUSIONS

The Co-doped VO_2 (B)has been prepared by one step hydrothermal synthesis method. Results show that proper Co doping is an effective method to improve its electrochemical performances, such as larger lithium-ion diffusion coefficients, higher electrochemical reversibility, and lower electrochemical reaction resistance. In particular, when doping amount of Co is x=0.02, the cathodes exhibited an excellent cycling performance. The capacity retention rate is 54.1% after 100 cycles, which is much higher than 48.0% of the pure VO_2 (B) sample. Improvement of electrochemical performance of the Co-doped VO_2 (B) samples could be attributed to the following reasons: first, the presence of more lower valence Co^{2+} can improve the conductivity of the electrode; secondly, the occupancy of Co^{2+} could stabilize the [VO_6] layers; last but not least, those local structural defects due to oxygen vacancies may benefit the fast intercalation/extraction of Li^+ in the layers of VO_2 (B).

ACKNOWLEDGEMENTS
This work was supported by the Nature Science Foundation of Wanjiang University of Technology, (No. WG18023ZD).

References

1. B. Dunn, H. Kamath and J.-M. Tarascon, *Science*, 334 (2011) 928.
2. N. Liu, H. Wu, M. T. McDowell, Y. Yao, C. Wang and Y. Cui, *Nano lett*., 12 (2012) 3315.
3. J. B. Goodenough and Y. Kim, *Chem. Mater*., 22 (2010) 587.
4. M. M. Thackeray, C. Wolverton And E. D. Isaacs, *Energy Environ. Sci*., 5 (2012) 7854.
5. H. Ren, R. Yu, J. Wang, Q. Jin, M. Yang, D. Mao, D. Kisailus, H. Zhao and D. Wang, *Nano lett*., 14 (2014) 6679.
6. J. Wang, N. Yang, H. Tang, Z. Dong, Q. Jin, M. Yang, D. Kisailus, H.Zhao, Z. Tang and D. Wang, *Angew. Chem. Int. Ed*., 52 (2013) 6417.
7. X. Lai, J. E. Halpert and D. Wang, *Energy Environ. Sci*., 5 (2012) 5604.
8. S. Xu, C. M. Hessel, H. Ren, R. Yu, Q. Jin, M. Yang, H. Zhao and D. Wang, *Energy Environ. Sci.,* 7 (2014) 632.
9. A. Pan, H. B. Wu, L. Yu and X. W. D. Lou, *Angew. Chem. Int. Ed*., 125 (2013) 2282.
10. R. Cava, A. Santoro, D. Murphy, S. Zahurak, R. Fleming, P. Marsh and R. Roth*, J. Solid State Chem.,* 65 (1986) 63.
11. X.F. Zhang, K.X. Wang, X. Wei and J.S. Chen, *Chem. Mater*., 23 (2011) 5290.
12. C. Nethravathi, C. R. Rajamathi, M. Rajamathi, U.K. Gautam, X. Wang, D. Golberg and Y. Bando, *ACS Appl. Mater. Interfaces*, 5 (2013) 2708.
13. S. Yang, Y. Gong, Z. Liu, L. Zhan, D. P. Ma, L.R. Vajtai and P. M. Ajayan, *Nano Lett*. 13 (2013) 1596.
14. C. Niu, J. Meng, C. Han, K. Zhao, M. Yan and L. Mai, *Nano Lett*. 14 (2014) 2873.
15. G. Ren, M. N. F. Hoque, X. Pan, J. Warzywoda and Z. Fan, *J. Mater. Chem.* A, 3 (2015) 10787.
16. S. Lee, X. G. Sun, A. A. Lubimtsev, X. Gao, P. Ganesh, T. Z. Ward, G. Eres, M. F. Chisholm, S. Dai and H. N. Lee, *Nano Lett.,*17 (2017) 2229.
17. D. Chao, C. Zhu, X. Xia, J. Liu, X. Zhang, J. Wang, P. Liang, J. Lin, H. Zhang, Z. X. Shen and H. J. Fan, *Nano Lett*.,15 (2015) 565.
18. P. Liu, Y. Xu, K. Zhu, K. Bian, J. Wang, X. Sun, Y. Gao, H. Luo, L. Lu and J. Liu, *J. Mater. Chem*. A, 5(2017) 8307.

19. Q. Liu, G. Tan, P. Wang, S. C. Abeyweera, D. Zhang, Y. Rong, Y. A. Wu, J. Lu, C.J. Sun, Y. Ren, Y. Liu, R. T. Muehleisen, L. B. Guzowski, J. Li, X. Xiao and Y Sun, *Nano Energy*, 36 (2017) 197.
20. P. Liu, Y. Xu, K. Zhu, K. Bian, J. Wang, X. Sun, Y. Gao, H. Luo, L. Lu and J. Liu, *J. Mater. Chem. A*, 5 (2017) 8307.
21. J.F. Liu, Q.H. Li, T.H. Wang, D.P. Yu And Y.D. Li, *Angew. Chem. Int. Ed*., 43 (2004) 5048.
22. W. Chen, J.F. Peng, L.Q. Mai, H. Yu and Y.Y. Qi, *Chem. Lett.,* 33 (2004) 1366.
23. X.Y. Chen, X. Wang, Z.H. Wang, J.X. Wan, J.W. Liu and Y.T. Qian, *Nanotechnology*,15 (2004) 1685.
24. R. Li and C.Y. Liu, *Mater. Res. Bull*., 45 (2010) 688.
25. W.W Han, H.Q Chu, Y.C Ya, S.L Dong and C. Zhang. *Fuller. Nanotube Car. N*., 27 (2019)265.
26. H.Q Chu, W.W Han, F. Ren, L.K Xiang, Y. Wei and C. Zhang. *ES Energy Environ*., 2 (2018) 73.
27. Z.G. Zou, S.C. Han, Y.W. Li, X.Y. Wu, Q. Yang and T.T. Lv, *Int. J. Electrochem. Sci.,* 13 (2018) 8127.
28. Théobald F. Theobald, R. Cabala and J. Bernard, *J. Solid State Chem*., 17 (1976) 431.
29. X. Sun and Y. Li, *Angew. Chem. Int. Ed*., 43 (2004) 597.
30. T.R. Gilson, O.F. Bizri and N. Cheetham, *J. Chem. Soc.,* 3(1973) 291.
31. J. Jin, X. Fu, Q. Liu, Y. Liu, Z. Wei, K. Niu and J. Zhang, *ACS Nano*, 7 (2013) 4764.
32. W. Li, J. Liu and C. Yan, *Carbon*, 49 (2011) 3463.
33. M. Oku, K. Hirokawa and *J. Electron Spectrosc. Relat. Phenom*., 8 (1976) 475.
34. X.H. Liu, G. Xie, C. Huang, Q. Xu, Y. Zhang and Y. Luo, *Mater. Lett*., 62 (2008) 1878.
35. Q.L. Wei, Z.Y. Jiang, S.S. Tan, Q.D. Li, L. Huang, M.Y. Yan, L. Zhou, Q.Y. An and L.Q. Mai, *ACS Appl. Mater. Interfaces*, 7 (2015) 18211.
36. X .Chen, X. Wang and Z. Wang, *Nanotechnology*, 15 (2004) 1685.
37. Q.H.Wu, A.Thissen and W. Jaegermann, *Appl. Surf. Sci*., 250 (2005) 57.
38. F. Sediri, F.Touati and Gharbi N, *Materials Science and Engineering B:Solid- State Materials for Advance Technology,* 129 (2006) 251.
39. X.H. Rui, N. Ding, J. Liu, C. Li and C.H. Chen, *Electrochim. Acta,* 55 (2010) 2384.
40. Z.G. Zou, Z.L. Hou, J.L. Wang, Y. Gao, Z.D. Wan, S.C. Han, *Int. J. Electrochem. Sci.*,12 (2017) 4979.
41. H. Cheng, *Guilin, Guilin University of Technology,* (2014).